Available online at www.sciencedirect.com
ScienceDirect
Polymer 48 (2007) 512–521
polymer
www.elsevier.com/locate/polymer

Morphology, polymorphism behavior and molecular orientation of electrospun poly(vinylidene fluoride) fibers

Wu Aik Yee [a], Masaya Kotaki [b,1], Ye Liu [b], Xuehong Lu [a,*]

[a] School of Materials Science and Engineering, Nanyang Technological University, 50 Nanyang Avenue, Singapore 639798
[b] Institute of Materials Research and Engineering, 3 Research Link, Singapore 117602

Received 1 August 2006; received in revised form 9 November 2006; accepted 18 November 2006
Available online 5 December 2006

Abstract

The morphology, polymorphism behavior and molecular orientation of electrospun poly(vinylidene fluoride) (PVDF) fibers have been investigated. We found that electrospinning of PVDF from its *N*,*N*-dimethylformamide/acetone solutions led to the formation of β-phase. In contrast, only α- and γ-phase was detected in the spin-coated samples from the same solutions. In the aligned electrospun PVDF fibers obtained using a rotating disk collector, the β-phase crystallites had a preferred orientation along the fiber axis. The degree of orientation did not, however, vary significantly with the speed of the rotation disk collector, and the β-phase was also not significantly enhanced with the increase in the rotation speed or the decrease in the size of spinnerets. These facts indicated that the orientation was likely to be caused by Columbic force rather than the mechanical and shear forces exerted by the rotating disk collector and spinnerets. The Columbic force may induce local conformational change to straighter TTTT conformation, and hence promote the β-phase. The addition of 3 wt.% of tetrabutylammonium chloride (TBAC) into the polymer solutions effectively improved the morphology of the electrospun fibers, and led to almost pure β-phase in the fibers. With spin coating, PVDF–TBAC did not, however, show any strong β-phase diffraction peak. The synergistic β-enhancement effect of TBAC and electrospinning is possibly due to the fact that while TBAC could induce more *trans* conformers, electrospinning promotes parallel packing, and hence inter-chain registration.

Keywords: Poly(vinylidene fluoride) (PVDF); Electrospinning; Polymorphism

1. Introduction

Poly(vinylidene fluoride) (PVDF) has drawn great attention in recent years due to its attractive properties such as piezo-, pyro- and ferroelectricity, as well as flexibility, light weight and good processability. Although PVDF has a simple chemical structure, it is well established that it can exhibit five different polymorphs depending on its processing conditions. These crystal forms involve three different chain conformations, namely: (1) all-*trans* (TTTT) planar zigzag for β-phase, (2) TGTG′ for α and δ phases, and (3) T_3GT_3G' for γ and ε phases [1]. When PVDF chains are packed into crystal lattices, their dipoles are either additive, which leads to a net dipole as in β, γ and δ phases, or canceled among themselves, resulting in no net dipole as in α and ε phases [1]. Among the three polar phases, the β-phase has the largest spontaneous polarization (p) per unit cell and thus exhibits the highest piezo-, pyro- and ferroelectric activities, which endues PVDF with great potentials for various device applications [2,3].

When PVDF is cooled from melt, it normally crystallizes in the non-polar α-phase. The polar β-phase can be obtained through various post-treatments of the melt-processed samples, such as mechanical stretching of melt-spun films/fibers in a certain temperature range [4–6] and thermal, corona or high-field room-temperature poling of the α-phase thin films [5–9]. The β-phase can also be induced directly under some special conditions, such as by melt crystallization at high pressure [10], in the process of vapor deposition of oligomeric PVDF [11,12], or by blending with carbon nanotubes [13]

* Corresponding author. Tel.: +65 6790 4585; fax: +65 6790 9081.
E-mail address: asxhlu@ntu.edu.sg (X. Lu).
[1] Present address: Division of Advanced Fibro Science, Kyoto Institute of Technology, Matsugasaki, Sakyo-ku, Kyoto 606-8585, Japan.

0032-3861/$ - see front matter © 2006 Elsevier Ltd. All rights reserved.
doi:10.1016/j.polymer.2006.11.036

and organically modified nanoclay [14–16]. When deposited from solutions PVDF commonly crystallizes in the α- and γ-form [17]. The β-phase has been found in solvent-cast thin films when a highly polar but toxic solvent, hexamethyl phosphoramide, was used [18], or hygroscopic/hydrated salts were added in the solutions as additives [19].

Electrospinning has been established as a simple and versatile method for drawing polymer fibers with diameters at nanometer- or submicron-scale [20–22]. The technique has been applied to fabricate PVDF nanofibers and fibrous thin films for various applications [23–26]. A previous study has shown that electrospun PVDF fibers can be semi-crystalline [26] while their polymorphic behavior has not been studied, and consequently, their electroactive properties have not been explored. This work was undertaken to investigate the crystalline phase variation in PVDF fibers electrospun under various conditions. We found that electrospinning of PVDF from its *N*,*N*-dimethylformamide/acetone solutions led to the formation of β-phase. In particular, with the addition of a small amount of tetrabutylammonium chloride (TBAC) into the PVDF solutions, the β-phase became dominant in the electrospun fibers. In contrast, for the spin-coated samples although the addition of TBAC led to a significant increase in *trans* conformers it did not promote long-range order impressively. It is believed that while TBAC induced local conformational changes electrospinning played a critical role in promoting inter-chain registration. Molecular orientation in the electrospun fibers was also examined and correlated to the polymorphism behavior of the fibers.

2. Experimental

2.1. Materials

PVDF powders (Solef 11008) was used as received. *N*,*N*-Dimethylformamide (DMF), acetone and acetic acid were supplied by Aldrich, and TBAC by Fluka.

2.2. Electrospinning

DMF/acetone mixtures were prepared at DMF/acetone weight ratio of 60/40, 70/30 and 80/20, respectively. PVDF was dissolved in the solvent mixtures at PVDF concentration, namely polymer/solvent weight ratio, of 15 and 20 wt.%, respectively. The PVDF solutions were then placed in a plastic syringe fitted with a needle of tip-diameter of 200, 30 and 1 μm, respectively. PVDF fibers were electrospun at 15 or 21 kV with a high-voltage power supply. A syringe pump was used to feed the polymer solution into the needle tip, and the feed rate of the syringe pump was fixed at 0.25 ml/h. A grounded aluminum foil was located at a fixed distance of 15 cm from the needle tip to collect the fibers. The fibers were randomly deposited on the collector plate forming a fibrous thin film (random mat). In parallel to the above, 3 wt.% of acetic acid and TBAC (the mass of the additive/the mass of solvents) were added into the 20 wt.% PVDF polymer solution (DMF/acetone = 60/40), respectively, and the solutions were electrospun at 21 kV using the 27G needle (tip-diameter = 200 μm). The 20 wt.% PVDF polymer solutions, with and without TBAC, were also electrospun at 15 kV using the setup shown in Ref. [24]. The fibers were collected using the setup shown in Ref. [27] at the rotating disk speed of 600, 1000, 1500 and 2000 rpm, respectively, with the fibers aligning in the rotation direction. All electrospun fibers were dried *in vacuo* at room temperature overnight prior to characterization.

2.3. Spin-coating

The 20 wt.% PVDF solutions in 60/40 DMF/acetone mixture, with and without 3 wt.% TBAC, were spin-coated at 2000 rpm using a Cost Effective Equipment (CEE) Model 100 spin-coater. The thin films obtained were dried *in vacuo* at room temperature overnight prior to characterization.

2.4. Scanning electron microscopy (SEM)

The morphology of the electrospun fibers was examined using *a JEOL 5600* SEM. A thin layer of gold was sputtered on the sample surface before the examination.

2.5. Wide angle X-ray diffraction (WAXD)

WAXD patterns were recorded with a Bruker GADDS X-ray diffractometer equipped with a two-dimensional (2D) area detector using Cu Kα radiation. The random mats were rolled to make tubes of ~1 mm diameter for the X-ray measurement while the aligned samples were measured directly without rolling, as shown in Fig. 1. For all samples, 2D diffraction patterns were collected in the 2θ range of 15°–50°, and integrated to obtain azimuthal average intensity against 2θ plots using GADDS software package. To examine crystal orientation, the same software was used to obtain the radial average intensity of equatorial reflections versus azimuthal angle (χ) plots.

2.6. Differential scanning calorimetry (DSC)

The DSC curves of the materials were measured using a TA Instruments Modulated DSC 2920. The sample was heated at 20 °C/min from 25 to 200 °C. All experiments were performed under a nitrogen purge.

2.7. Attenuated Fourier transform infrared spectroscopy (AT-FTIR)

FTIR spectra were collected using a Perkin Elmer FTIR System Spectrum GX equipped with a Golden Gate Single

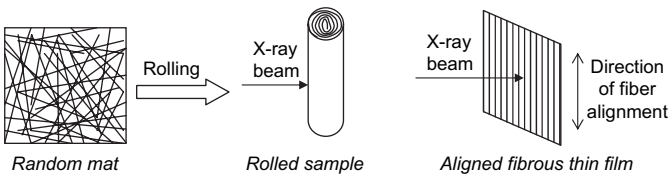

Fig. 1. A schematic of the geometries of the WAXD experiments.

Diamond Attenuated Total Reflection (ATR) unit (Grasby Specac ATR 10500). The samples were placed on top of the ATR set and scanned from 4000 to 600 cm^{-1}. The incidence angle used was 45°. A total of 16 scans were collected for signal averaging.

3. Results and discussion

3.1. Electrospinning versus spin-coating

SEM micrographs of PVDF fibers prepared by electrospinning from 20 wt.% PVDF solutions in DMF/acetone with different DMF/acetone ratios are shown in Fig. 2. With the increase of the DMF/acetone ratio, the average fiber diameter was decreased while the population and size of beads were increased, which can be attributed to the higher polarity and boiling point of DMF over that of acetone [23,26].

Unlike the morphology, polymorphic behavior of the electrospun PVDF fibers did not vary with the DMF/acetone ratio, as indicated by the WAXD patterns of the fibers obtained at different DMF/acetone ratios (Fig. 3). In all the diffraction patterns there were apparently five peaks, and the positions and intensities of the peaks did not significantly vary with the DMF/acetone ratio. The presence of a very strong peak at $2\theta = 20.6°$, which corresponds to 200/110 reflections of the β-phase, and distinctive peaks at around 18.5° and 27.4° 2θ, which correspond to 020 and 111 reflections of the α-phase, respectively [28], indicated the co-existence of the α- and the β-phase in the electrospun PVDF fibers. This is corroborated by the FTIR spectrum of the fibers, shown as curve a in Fig. 4, where the α-phase related bands can be observed

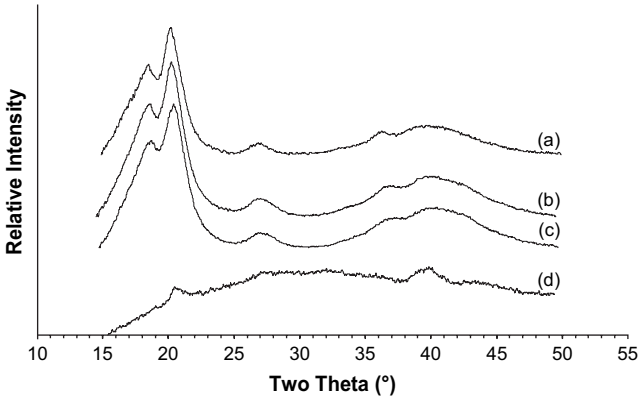

Fig. 3. WAXD patterns of PVDF fibers electrospun at 15 kV from PVDF in DMF/acetone solutions with DMF/acetone weight ratios of: (a) 80/20, (b) 70/30 and (c) 60/40; the samples were in the form of rolled random mats. (d) The WAXD pattern of the spin-coated PVDF film from PVDF in DMF/acetone solution with DMF/acetone weight ratio of 60/40. The PVDF concentration was 20 wt.% for all samples.

at 614, 765, 795 and 975 cm^{-1} and the β-phase related bands at 840 and 1278 cm^{-1} [29].

In contrast to the electrospun fibers, the spin-coated film exhibited very weak and broad diffraction peaks, which were due to the small size of the crystallites. Fig. 4 also shows that the relative intensities of the α-phase infrared absorption bands are slightly higher for the spin-coated sample (curve b in Fig. 4) than its electrospun counterpart (curve a in Fig. 4). In addition, the β-phase band at 1278 cm^{-1} is absent while a γ-phase related band appears at 1225 cm^{-1} for the spin-coated sample, which confirms that by spin-coating PVDF crystallizes mainly in the α- and γ-form from its solution in acetone/DMF [17].

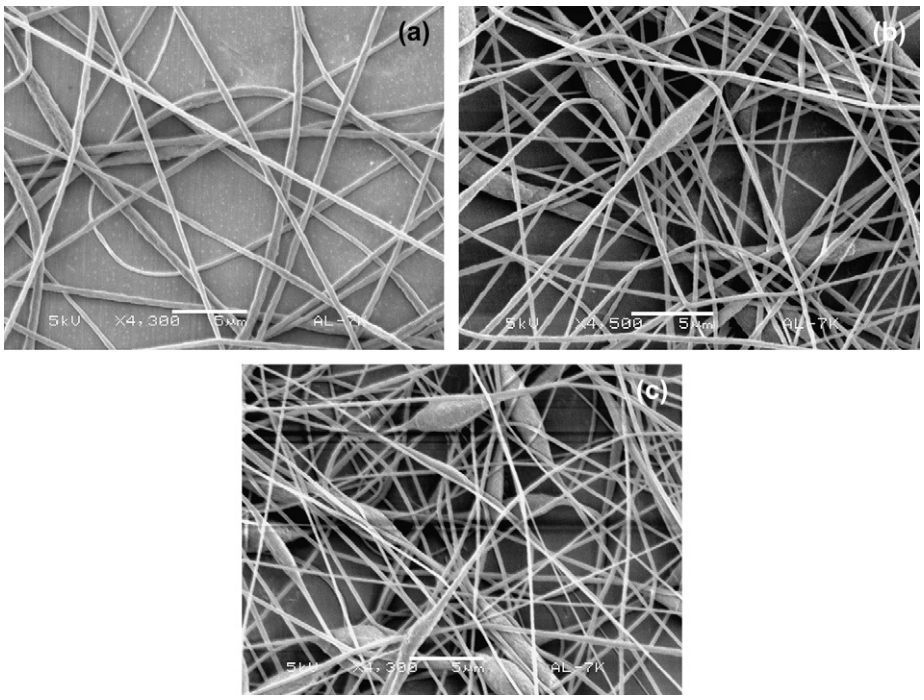

Fig. 2. SEM micrographs showing morphology of PVDF fibers electrospun at 15 kV from PVDF in DMF/acetone solutions with DMF/acetone weight ratios of: (a) 60/40, (b) 70/30 and (c) 80/20. The PVDF concentration was 20 wt.% for all samples.

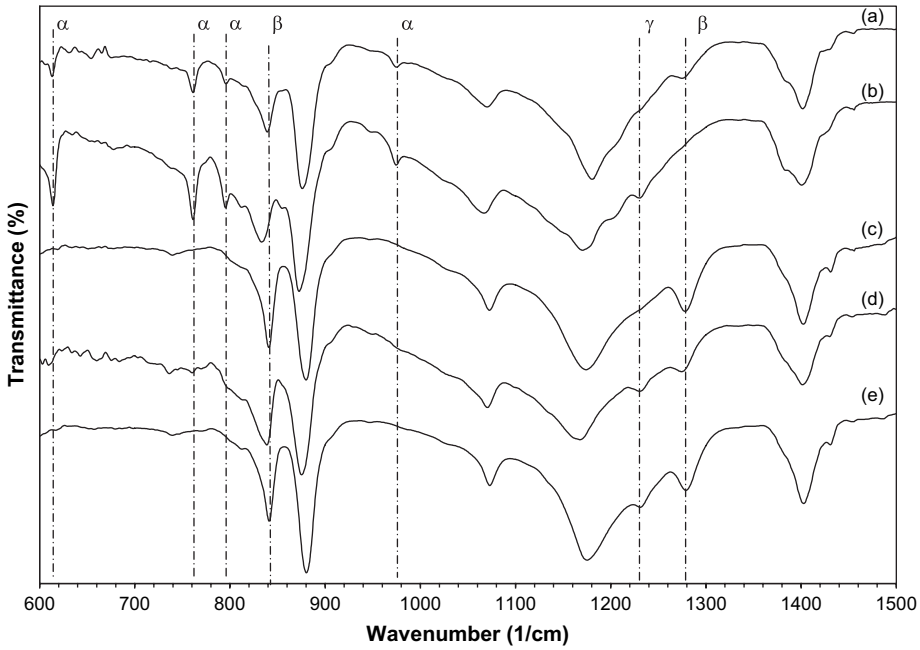

Fig. 4. FTIR spectra of: (a) PVDF fibers electrospun from a PVDF in DMF/acetone solution without TBAC, (b) PVDF film spin-coated from a PVDF in DMF/acetone solution without TBAC, (c) PVDF fibers electrospun from a PVDF in DMF/acetone solution with 3 wt.% TBAC, (d) PVDF film spin-coated from a PVDF in DMF/acetone solution with 3 wt.% TBAC and (e) PVDF fibers electrospun from a PVDF in DMF/acetone solution with 3 wt.% TBAC and collected using a rotation disk collector at 1500 rpm. The DMF/acetone ratio and PVDF concentration were 60/40 and 20 wt.% for all samples.

The above comparison between the electrospun and spin-coated samples demonstrated the effect of electrospinning in promoting the β-phase, which may be attributed to spinning-induced conformational change, *i.e.* change from TGTG′ and T_3GT_3G' to straighter TTTT conformation.

3.2. Crystal orientation

During electrospinning, a polymer solution experiences two forces. One is a shear force when it flows through a capillary (needle) at a very high rate. The other one is a Columbic force when the jet is elongated and accelerated by the high electric field applied. When a rotation disk collector is used to collect the fibers, a mechanical force may also be applied. The above three forces may cause polymer chains be aligned and/or stretched in the spinning direction. To study the role that each force plays, a rotating disk collector was used to collect electrospun PVDF fibers at various rotation speeds, and the morphology, orientation and polymorphism behavior of the aligned fibers were characterized.

When the rotation speed was less than 600 rpm, the fibers could not be effectively aligned in the rotation direction. With the rotation speed of 600 rpm or higher, we achieved the unidirectional alignment of PVDF fibers at very short collection time, as shown in Fig. 5(a). After a long period of collection with the rotating disk collector, although the electrospun fibers were still generally aligned in the rolling direction, there was a slight element of randomness in the fibrous thin film produced, as shown in Fig. 5(b). This could be due to the presence of residual charges on the electrospun fibers. When the collection time was short, the surface charges on the fibers repelled each other resulting in a wide space between each other. However, as the collection time increased, the accumulation of fibers resulted in an increase in this repelling force,

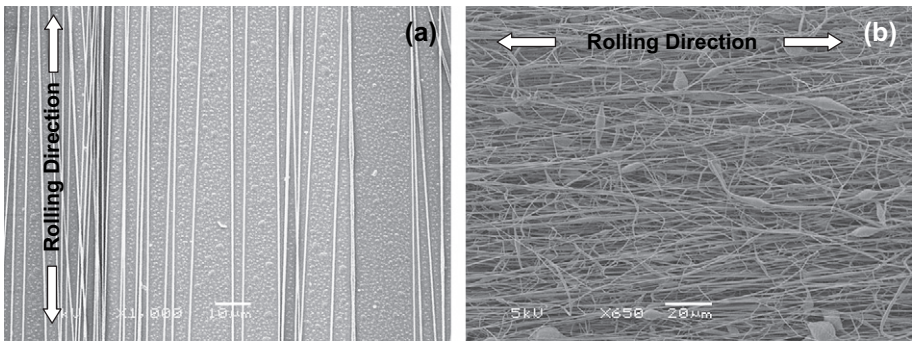

Fig. 5. SEM micrographs showing morphology of the electrospun PVDF fibers collected using the rotating disk collector at 1000 rpm for: (a) 10 s and (b) 5 min. The DMF/acetone ratio and PVDF concentration were 60/40 and 20 wt.% for both samples.

resulting in the fibers to be deposited in a direction slightly off the rolling direction.

Fig. 6 shows 2D WAXD patterns of the aligned PVDF fibers collected at the rotation speed of 1000 and 2000 rpm. Only equatorial areas are shown because the intensities for other reflections are too low to be seen clearly. In both patterns, the peak at $2\theta = 20.6^\circ$, which corresponds to 200/110 reflections of the β-phase, appears as an arc centered on the equator, while the intensity of the peak at $2\theta = 18.5^\circ$, which corresponds to 020 reflection of the α-phase, seems to be distributed uniformly along a ring. The difference between the two peaks can be seen more clearly from their radial average intensity versus azimuthal angle (χ) plots (Fig. 7). In Fig. 7(a), for the β-phase reflection there is a fairly sharp peak at $\chi = -90^\circ$ (equator) while for the α-phase reflection the intensity variation with the azimuthal angle is much smaller. This indicates that the *c*-axis of the β-phase crystallites has preferred orientation along the fiber axis while the α-phase crystallites have a much lower degree of orientation. The fact proves that the formation of the β-phase in electrospun PVDF fibers is closely related to the orientation and/or stretching of the chains along the fiber axis induced by the forces exerted in electrospinning.

From Fig. 7(b), it was observed that the degree of crystal orientation did not vary significantly with the speed of the rotation disk collector. The variation in the rotation speed also did not lead to significant enhancement of the β-phase, as demonstrated by the very slight variation of the intensity ratio of 020^{α}–$200/110^{\beta}$ diffraction peak with the rotation speed (Fig. 8 and Table 1). The combination of the above two facts implies that the β-phase is mainly induced by the forces applied during the spinning process rather than the mechanical force exerted by the rotation disk collector. The role of the mechanical force is mainly to align the fibers. There was only a very slight increase in crystallinity and melting temperature with the increase of the rotation speed, as shown in Table 1. The slightly increased crystallinity is likely to be contributed by the growth of γ-phase as evidenced by the appearance of

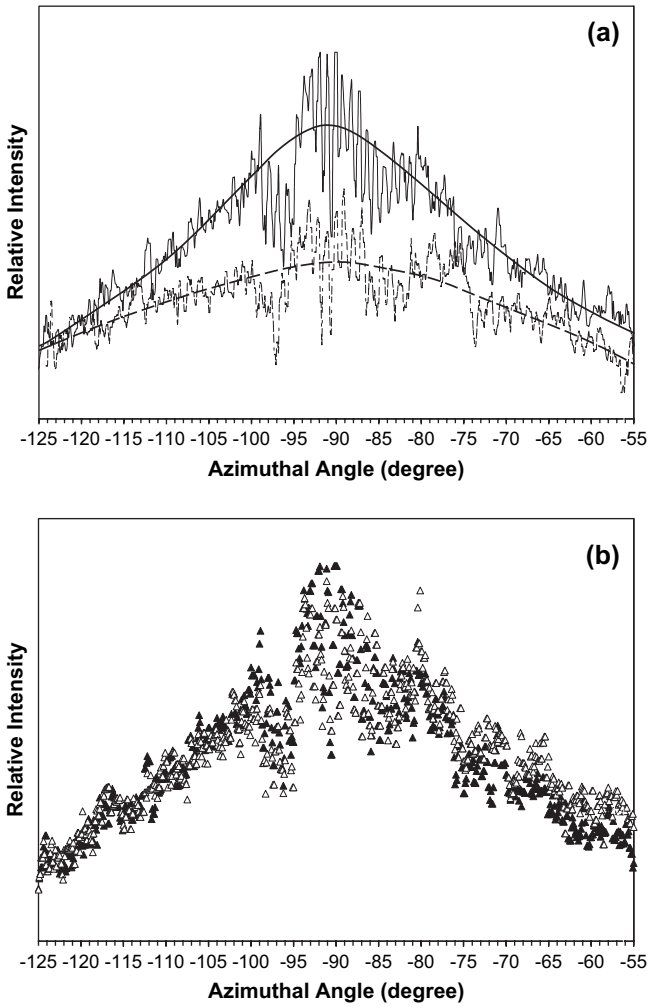

Fig. 7. Radial average intensity versus azimuthal angle plots obtained from scanning the 2D WAXD patterns in Fig. 6. (a) Intensity profiles of $200/110^{\beta}$ peak (solid line) and 020^{α} peak (dashed line); for both the rotation speed was 2000 rpm; the 2θ range was 18.0°–19.2° for the α peak and 19.6°–20.8° for the β peak. (b) Intensity profiles of the β peak for the fibers collected at the rotation speed of 1000 rpm (solid point) and 2000 rpm (void point).

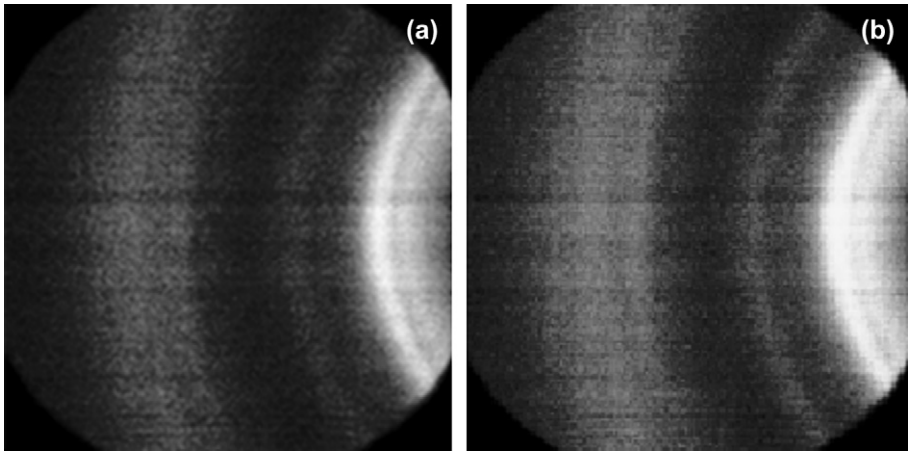

Fig. 6. 2D WAXD patterns of PVDF fibers electrospun at 15 kV from a PVDF in DMF/acetone solution and collected using the rotating disk collector at: (a) 1000 and (b) 2000 rpm. The DMF/acetone ratio and PVDF concentration were 60/40 and 20 wt.% for both samples.

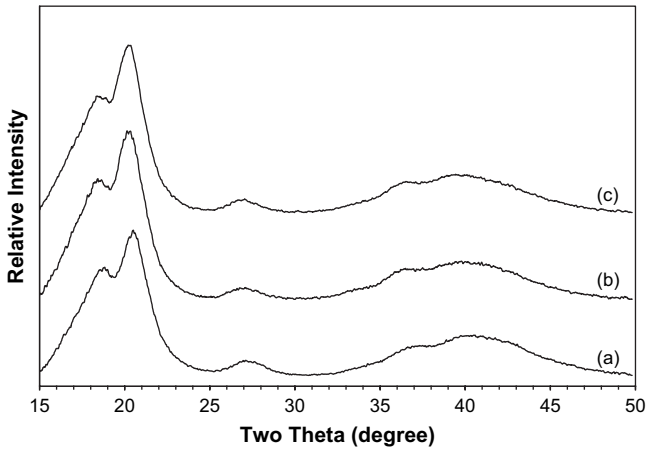

Fig. 8. WAXD patterns of the electrospun PVDF fibers collected using: (a) a static collecting plate, (b) the rotating disk collector at 1000 rpm and (c) the rotating disk collector at 2000 rpm. The voltage applied was 15 kV, and the DMF/acetone ratio and PVDF concentration were 60/40 and 20 wt.% for all samples.

Table 1
The intensity ratio of 020^{α}–$200/110^{\beta}$ diffraction peak, as well as the heat of fusion and peak melting temperature obtained from the 1st heating DSC curves, of electrospun PVDF fibers

Speed of the rotating disk collector (rpm)	Spinneret size (μm)	Intensity ratio of 020^{α}–$200/110^{\beta}$ diffraction peak	Heat of fusion (J/g)	Melting temperature (°C)
2000	200	0.70	47.3	157.0
1500	200	0.68	46.1	156.9
1000	200	0.71	46.1	156.6
–[a]	200	0.74	46.3	156.2
–[a]	30	0.69	47.3	157.1
–[a]	1	0.72	47.8	160.3

The DMF/acetone ratio and PVDF concentration were 60/40 and 20 wt.% for all samples.
[a] A static collecting plate was used.

a weak shoulder peak at about 19° 2θ for the fibers collected at 2000 rpm [28].

3.3. Micron-sized needles as the spinneret

The motivation of use of micron-sized needles as the spinneret was to increase the shear force in the capillary, and investigate whether it could promote the formation of the β-phase.

SEM micrographs of the PVDF fibers prepared by electrospinning from 15 wt.% PVDF solution in 80/20 DMF/acetone with different needle tip-size are shown in Fig. 9. A high population of beads was observed in the electrospun fibers when 27G needles ($D = 200$ μm) were used. By reducing the needle tip-diameter, the size of the beads was decreased and the shape of the beads became more elongated. The possible reasons for the phenomenon are that the dimension of the Taylor cone formed during the electrospinning becomes smaller and the surface tension is reduced [30].

Fig. 10 shows the WAXD patterns of the electrospun fibers using spinnerets of different size. Obviously the reduced needle diameter did not lead to significant enhancement of the β-phase, as demonstrated by the insignificant change in the intensity ratio of 020^{α}–$200/110^{\beta}$ diffraction peak with the spinneret size (Table 1). However, the use of 1 μm needle led to slight sharper peaks for all α and β reflections. The DSC data of the fibers (Table 1) indicated a slight increase in the heat of fusion as well as the melting temperature with the reduction in spinneret size. It implies that the increase of the shear force in the capillary may have led to a higher degree of disentanglement and parallel packing, which justifies the slightly higher crystallinity and larger crystal size, but relaxation, especially the conversion of *trans* conformers back to *gauche* conformers, occurred very quickly. Taking note of the ineffectiveness of the use of the rotation disk collector and micro-sized spinnerets in further enhancing the β-phase, the formation of the β-phase in the electrospun fibers is likely to be mainly brought by the Columbic force.

3.4. Effects of additives

For polymers that exhibit polymorphism, the inclusion of additives has often been found to exert an important effect on the type of crystal phase developed [14–16,31,32]. In this work, two polar compounds, acetic acid and tetrabutylammonium chloride (TBAC), were selected to be added into the polymer solutions mentioned above at a concentration of 3 wt.% (mass of additive/mass of solvents) to study their effects on morphology and polymorphism of the electrospun fibers. Both compounds were in free ion form to some extent in the DMF/acetone mixtures, which led to a tremendous increase in electrical conductivity of the solvents, as shown in Table 2. The conductivity increment became, however, much smaller after PVDF was dissolved in the solvent mixtures because the positive charged ions may interact strongly with fluorine atoms on the PVDF chains. Nevertheless the addition of TBAC into the PVDF solutions still brought about an increase in conductivity by three orders as compared to the increase of about 50% for the addition of acetic acid.

From the SEM micrographs shown in Fig. 11, we can see that the addition of acetic acid significantly reduced the density and size of the beads, while the addition of TBAC effectively removed all traces of beads from the electrospun fibers. The fiber diameter was reduced in both cases. The morphological improvement of the electrospun fibers can be attributed to the increase in the charge density of the polymer solutions [30].

The WAXD patterns of the fibers electrospun from the PVDF solutions containing acetic acid and TBAC are shown in Fig. 12. For the system with acetic acid, the diffraction pattern is very similar to that without any additive. This implies that the crystallization occurred after acetic acid had almost evaporated off. While for the system with TBAC, the absence of the α-phase peaks at 18.6° and 27.4° 2θ clearly signals out the dominance of the β-phase in the electrospun fibers. The above result agrees well with the FTIR spectrum of the PVDF/TBAC fibers, shown as curve c in Fig. 4, where the

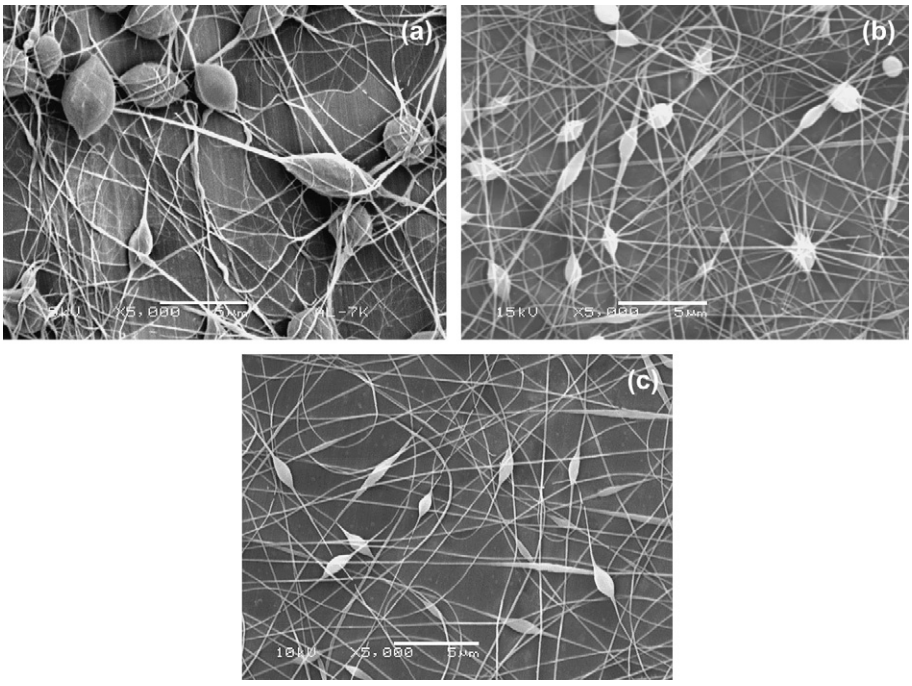

Fig. 9. SEM micrographs showing morphology of PVDF fibers electrospun at 15 kV from a PVDF in DMF/acetone solution using needles of diameter of: (a) 200 μm, (b) 30 μm and (c) 1 μm. The DMF/acetone ratio and PVDF concentration were 80/20 and 15 wt.% for all samples.

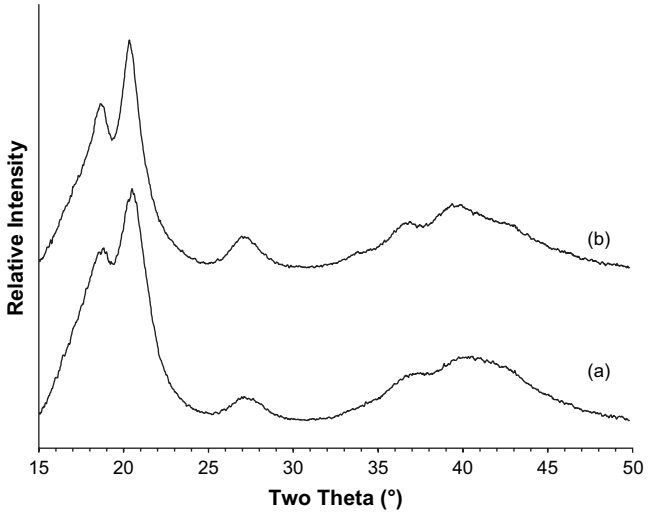

Fig. 10. WAXD patterns of PVDF fibers electrospun at 15 kV from PVDF in DMF/acetone solutions using needles of diameter of: (a) 200 μm and (b) 1 μm. The DMF/acetone ratio and PVDF concentration were 80/20 and 15 wt.% for all samples.

absence of the α-related bands at 614, 765, 795 and 975 cm^{-1} was observed.

A major difference between acetic acid and TBAC is that acetic acid evaporates off during the electrospinning process while TBAC molecules remain in the system. The β-phase enhancement effect induced by TBAC is likely to be caused by the hygroscopic nature of the salt, which retains water in the fibers and leads to hydrogen bonding between the water molecules and the fluorine atoms of PVDF [19]. An evidence for this is the appearance of a weak and broad infra absorption band at about 3400 cm^{-1}, as shown in Fig. 13, which is usually assigned to hydrogen-bonded N–H or O–H stretching vibration. As both PVDF and TBAC do not have N–H or O–H bonds, this broad peak is likely to be from the residue water in the system.

Table 2
Electrical conductivities of the solvents and polymer solutions

Solvent composition and additive	Conductivity without PVDF (μS/cm^2)	Conductivity with 20 wt.% PVDF (μS/cm^2)
DMF/acetone 60/40	1.6	2.6
DMF/acetone 60/40 + 3 wt.% acetic acid	10.2	4.1
DMF/acetone 60/40 + 3 wt.% TBAC	3770	1969

In contrast to the electrospun PVDF–TBAC fibers, but similar to the spin-coated PVDF film (without TBAC), the spin-coated PVDF–TBAC film exhibited very weak and broad diffraction peaks, as shown in Fig. 12(d). The FTIR spectrum of the spin-coated PVDF–TBAC film, given as curve d in Fig. 4, shows, however, the β-phase related band at 1278 cm^{-1}, which is not seen for the spin-coated PVDF film (curve b in Fig. 4). The above fact implies that with the spin-coating the addition of TBAC has induced more TTTT conformers but the crystallinity and crystal size, as measured by X-ray diffraction, are not increased. The apparent ''different'' observations obtained in WAXD and FTIR measurements arise because X-ray diffraction measures long-range order as a result of chain packing, while FTIR measures the concentration of the ''crystalline isomers'', which is in fact, a short-range order phenomenon. The presence of TTTT conformers is a necessary condition for the

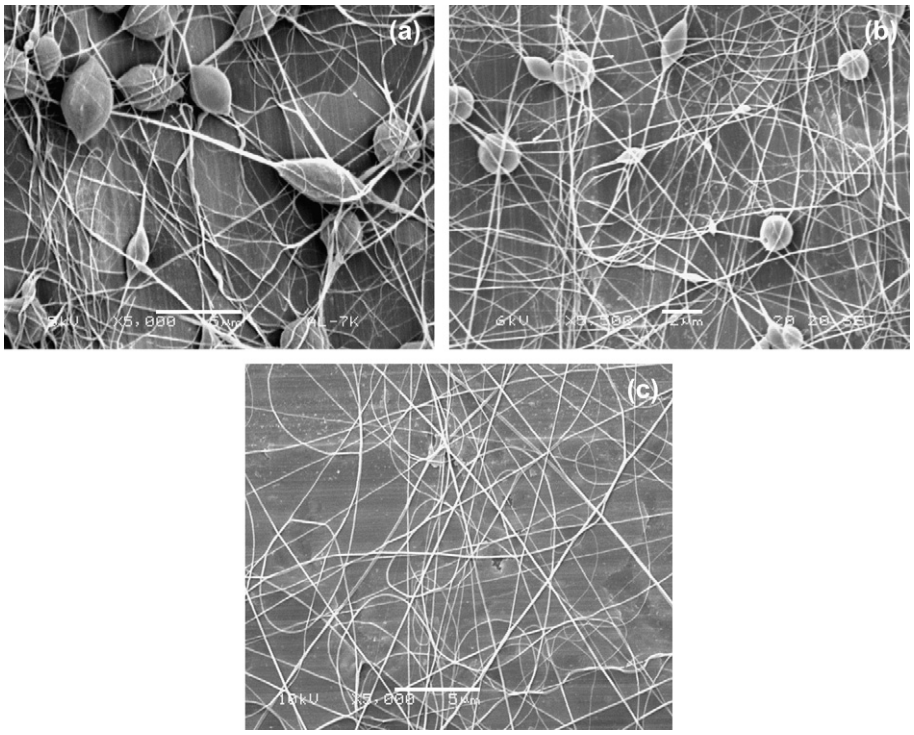

Fig. 11. SEM micrographs showing morphology of PVDF fibers electrospun at 15 kV from: (a) a PVDF in DMF/acetone solution without any additive, (b) a PVDF in DMF/acetone solution with 3 wt.% of acetic acid and (c) a PVDF in DMF/acetone solution with 3 wt.% of TBAC. The DMF/acetone ratio and PVDF concentration were 80/20 and 15 wt.% for all samples.

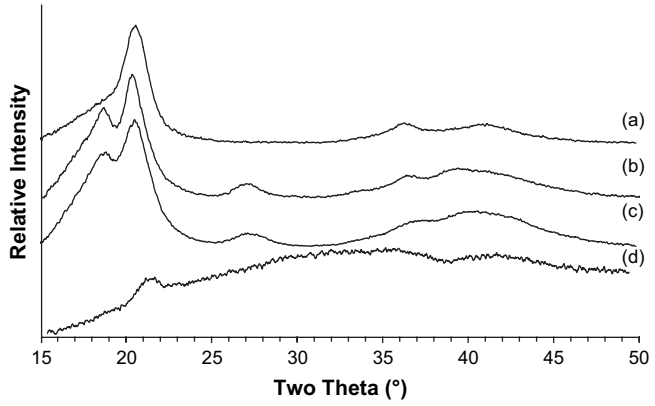

Fig. 12. WAXD patterns of: (a) PVDF fibers electrospun from a PVDF in DMF/acetone solution with 3 wt.% TBAC, (b) PVDF fibers electrospun from a PVDF in DMF/acetone solution with 3 wt.% acetic acid, (c) PVDF fibers electrospun from PVDF in DMF/acetone solution without any additive, and (d) PVDF film spin-coated from a PVDF in DMF/acetone solution with 3 wt.% TBAC. The DMF/acetone ratio and PVDF concentration were 60/40 and 20 wt.% for all samples.

β-phase to be present, but the TTTT conformers may exist without the presence of long-range order, as inter-chain registration is the dominant factor for the formation of stable β-phase nuclei from the highly entangled polymer solutions. Although the interaction between fluorine atoms and water may have induced more TTTT conformers in the spin-coated PVDF–TBAC film, the long-range order was not well established as such molecular interaction was ineffective in promoting inter-chain registration. Unlike the spin-coated PVDF–TBAC sample, in the electrospun PVDF–TBAC fibers the local conformational change was induced by TBAC while the development of long-range order was promoted by electrospinning, *i.e.* the addition of TBAC and electrospinning had synergistic β-enhancement effect. The role of electrospinning played in this case is mainly inducing disentanglement and parallel packing and hence facilitating inter-chain registration.

Fig. 14 shows the 2D WAXD pattern of the electrospun PVDF–TBAC fibers collected using the rotating disk collector at 1500 rpm. The strongest reflection was clearly an arc centered on the equator, which again proved the preferred orientation of the *c*-axis of the β crystallites along the fiber axis.

Fig. 15(a) compares the WAXD patterns of the electrospun PVDF–TBAC fibers collected with and without the use of the rotating disk collector. The absence of the α-phase peak at $2\theta = 27.4^\circ$ indicated the dominance of the β-phase in both cases. The fibers collected using the rotating disk collector showed an additional weak shoulder peak at $2\theta = 19.2^\circ$, which is likely to be a γ-phase peak [28]. FTIR spectra of the random PVDF–TBAC fibrous thin film and the aligned PVDF–TBAC fibers collected at 1500 rpm are given as curves c and e in Fig. 4. The difference between the two spectra is that an additional band appears at about 1225 cm^{-1} for the fibers collected using the rotating disk collector, which is a characteristic γ-phase band. This verified that when TBAC was added into PVDF solutions, the γ-phase was promoted slightly by using the rotating disk collector. It is worth noting that with the

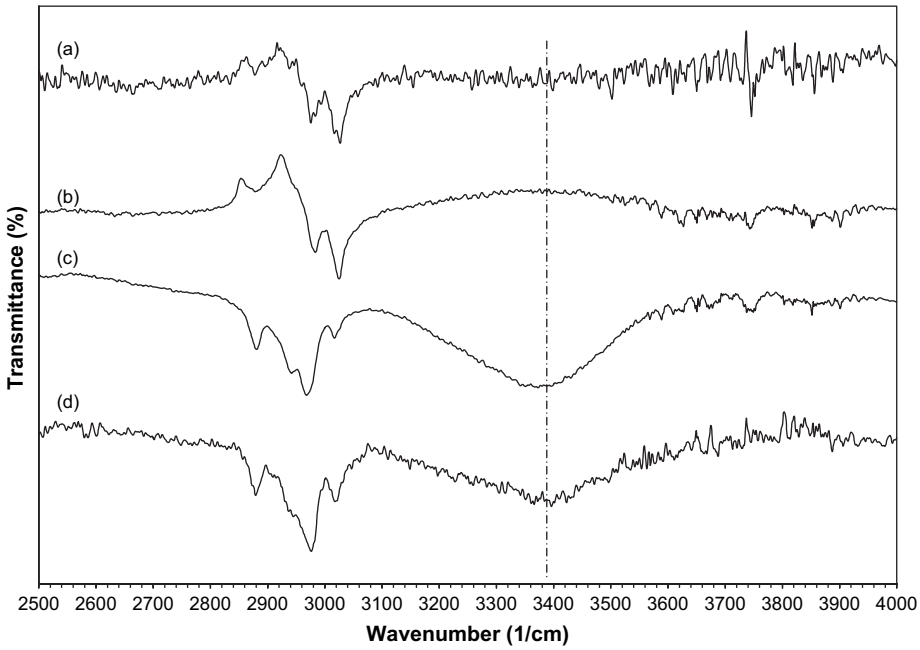

Fig. 13. FTIR spectra of: (a) PVDF fibers electrospun from a PVDF in DMF/acetone solution without TBAC, (b) PVDF film spin-coated from a PVDF in DMF/acetone solution without TBAC, (c) PVDF fibers electrospun from a PVDF in DMF/acetone solution with 3 wt.% TBAC and (d) PVDF film spin-coated from a PVDF in DMF/acetone solution with 3 wt.% TBAC in the O–H and C–H mode regions. The DMF/acetone ratio and PVDF concentration were 60/40 and 20 wt.% for all samples.

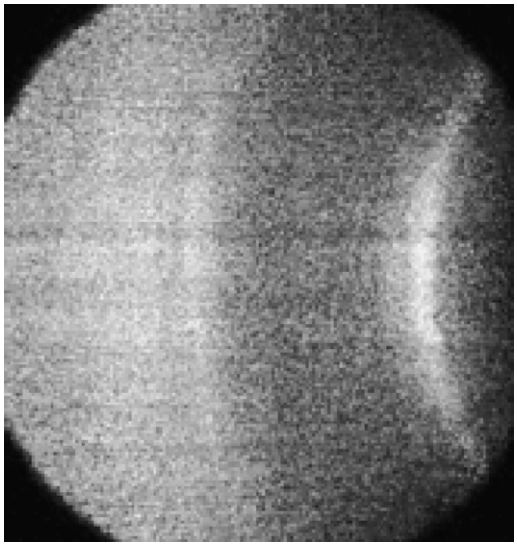

Fig. 14. Two-dimensional WAXD pattern of the aligned fibers electrospun at 15 kV from a PVDF in DMF/acetone solution with 3 wt.% TBAC and collected using the rotating disk collector at 1500 rpm. The DMF/acetone ratio and PVDF concentration was 60/40 and 20 wt.%, respectively.

addition of TBAC, the crystallinity was in general reduced due to the hindrance effect of the additive. Fig. 15(b) shows that the use of the rotating disk collector resulted in a small increase in the heat of fusion (from 28.2 to 31.4 J/g) and melting temperature as compared to that of PVDF–TBAC random mats, which signals an increase in crystallinity and crystal size. The increased crystallinity is likely to be contributed by the growth of γ-phase, as discussed above.

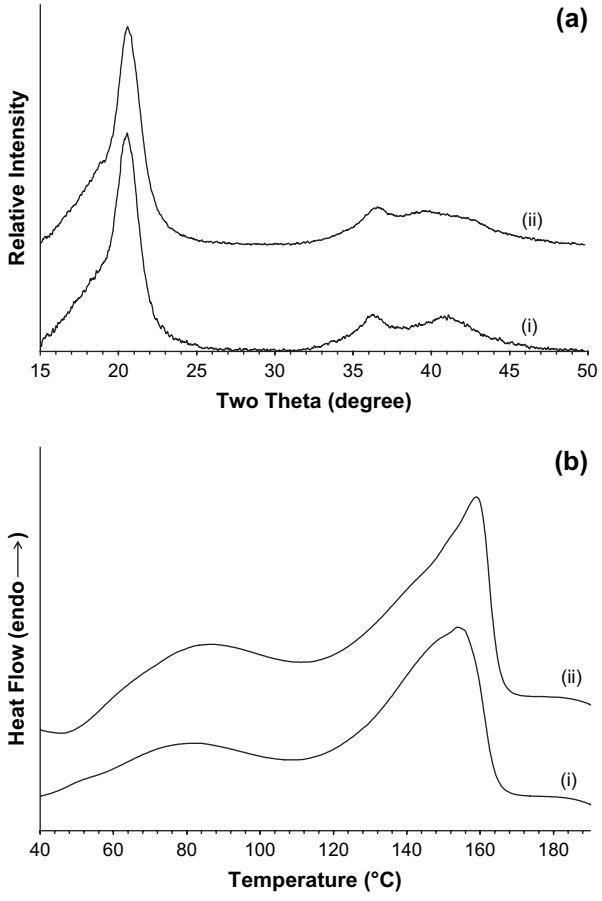

Fig. 15. (a) WAXD patterns and (b) the 1st heating DSC curves of the electrospun PVDF–TBAC fibers collected using (i) a static plate collector and (ii) the rotating disk collector at 1500 rpm. The DMF/acetone ratio and PVDF concentration were 60/40 and 20 wt.% for both samples.

4. Conclusions

1. Electrospinning of PVDF from its DMF/acetone solutions promoted the formation of the β-phase. In contrast, only the α- and γ-phase was detected in the spin-coated samples from the same solutions. The DMF/acetone ratio affected the fiber morphology significantly but did not alter polymorphic behavior of the PVDF fibers.
2. In the aligned electrospun PVDF fibers, the *c*-axis of the β-phase crystallites had preferred orientation along the fiber axis. The degree of orientation and the polymorphism behavior of the fibers did not, however, vary significantly with either the rotating disk speed or the size of the spinneret used. This implies that the formation of the β-phase is likely to be caused by the Columbic force imposed by the electric field rather than the mechanical and shear force exerted by the rotation disk collector and spinnerets. The Columbic force may cause conformational changes to straighter TTTT conformation, and hence promote the β-phase.
3. The addition of 3 wt.% of TBAC into the polymer solutions can effectively improve the morphology of the electrospun fibers due to the great increase in the conductivity of the solutions, and lead to almost pure β-phase in the fibers. With spin-coating, PVDF–TBAC did not, however, show any strong β-phase diffraction peak. The synergistic β-enhancement effect of TBAC and electrospinning is possibly due to that TBAC, a hygroscopic salt, could retain water in the fibers, which may lead to hydrogen bonding between the water molecules and the fluorine atoms of PVDF and hence more *trans* conformers, while electrospinning-induced disentanglement and parallel packing, and hence promoted inter-chain registration.

Acknowledgment

Wu Aik Yee thanks Singapore Economic Development Board (EDB) and Nanyang Technological University (NTU) for providing his scholarship in the course of this work.

References

[1] Tahiro T. In: Nalwa HS, editor. Ferroelectric polymers: chemistry, physics and applications. New York: Marcel Dekker Inc.; 1995 [chapter 2].
[2] Cross LE. Mater Chem Phys 1996;43:108.
[3] Hidaka T, Minamide H, Ito H, Nishizawa J, Tamura K, Ichikawa S. J Lightwave Technol 2005;23(8):2469.
[4] Humphreys J, Ward IM. J Appl Polym Sci 1985;30:4069.
[5] Humphreys J, Lewis ELV, Ward IM. J Polym Sci Part B Polym Phys 1988;26:141.
[6] Sajkiewicz P, Wasiak A, Gocłowski Z. Eur Polym J 1998;35:423.
[7] Southgate PD. Appl Phys Lett 1976;28:250.
[8] Bamji SS, Kao KJ, Perlman MM. J Polym Sci 1980;18:1945.
[9] Mckinney JE, Davis GT, Broadhurst MG. J Appl Phys 1980;51:1676.
[10] Hattori T, Hikosaka M, Ohigashi H. Polymer 1996;37:85.
[11] Takeno A, Okui N, Kitoh T, Muraoka M, Umemoto S, Sakai T. Thin Solid Films 1991;202:205.
[12] Noda K, Ishida K, Horiuchi T, Matsushige K, Kubono A. J Appl Phys 1999;86:3688.
[13] Levi N, Czerw R, Xing S, Iyer P, Carroll DL. Nano Lett 2004;4:1267.
[14] Priya L, Log JP. J Polym Sci Part B Polym Phys 2002;40:1682.
[15] Priya L, Log JP. J Polym Sci Part B Polym Phys 2003;41:31.
[16] Shah D, Maiti P, Gunn E, Schmidt DF, Jiang DD, Batt CA, et al. Adv Mater 2004;16:1173.
[17] Prest WM, Luca DJ. J Appl Phys 1978;49:5042.
[18] Kobayashi M, Tashiro K, Tadokoro H. Macromolecules 1975;8:158.
[19] Benz M, Euler WB, Gregory OJ. Macromolecules 2002;35:2682.
[20] Deitzel JM, Kleinmeyer J, Harris D, Tan NCB. Polymer 2001;42(1):261–72.
[21] Theron SA, Zussman E, Yarin AL. Polymer 2004;45(6):2017–30.
[22] Lyons J, Li C, Ko F. Polymer 2004;45(22):7597–603.
[23] Won SW, Jo SM, Lee WS, Kim YR. Adv Mater 2003;15:2027.
[24] Kim JR, Choi SW, Jo SM, Lee WS, Kim BC. Electrochim Acta 2004;50:69.
[25] Dersch R, Steinhart M, Boudriot U, Greiner A, Wendroff JH. Polym Adv Technol 2005;16:276.
[26] Zhao Z, Li J, Yuan X, Li X, Zhang Y, Sheng J. J Appl Polym Sci 2005;97:466.
[27] Theron A, Zussman E, Yarin AL. Nanotechnology 2001;2:384–90.
[28] Esterly DM, Love BJ. J Polym Sci Part B Polym Phys 2004;42:91.
[29] Bormashenko Y, Pogreb R, Stanevsky O, Bormashenko E. Polym Test 2004;23:791.
[30] Li D, Xia Y. Adv Mater 2004;16:1151.
[31] Zheng W, Lu X, Toh CL, Zheng TH, He C. J Polym Sci Part B Polym Phys 2004;42:1810.
[32] Chua YC, Lu X, Wan T. J Polym Sci Part B Polym Phys 2006;44:1040.